Geology

Fluid flow along potentially active faults in crystalline rock

Colleen A. Barton, Mark D. Zoback and Daniel Moos

Geology 1995;23;683-686
doi: 10.1130/0091-7613(1995)023<0683:FFAPAF>2.3.CO;2

Notes

Fluid flow along potentially active faults in crystalline rock

Colleen A. Barton
Mark D. Zoback
Daniel Moos
Department of Geophysics, Stanford University, Stanford, California 94305

ABSTRACT

The relationship between in-situ stress and fluid flow in fractured and faulted rock is examined by using data from detailed analyses of stress orientation and magnitude, fracture geometry, and precision temperature logs that indicate localized fluid flow. Data obtained from three boreholes that penetrate highly fractured and faulted crystalline rocks indicate that potentially active faults appear to be the most important hydraulic conduits in situ. The data indicate that the permeability of critically stressed faults is much higher than that of faults that are not optimally oriented for failure in the current stress field.

INTRODUCTION

Fractures and faults provide permeable pathways for fluids at a variety of scales, from great depth in the crust to flow through fractured aquifers, geothermal fields, and hydrocarbon reservoirs. Fracture-enhanced permeability depends on fracture density, orientation, and, most important, the hydraulic conductivity of the different fracture and fault planes present. Although it is well known that relatively few fractures and faults in fractured rock masses often serve as the primary conduits for fluid flow (e.g., Long et al., 1991), the reasons some fractures and faults are much more permeable than others are poorly understood.

In an arbitrarily fractured medium, the fracture population is often composed of fractures at various orientations. Subsets of this population could be extensile fractures, oriented perpendicular to the least principal stress (e.g., Pollard and Aydin, 1988); shear fractures, potentially active faults in the current stress field; or neither, faults and fractures whose orientations bear no apparent relation to the current stress field. In this paper, we use data from boreholes that penetrate highly fractured and faulted crystalline rocks to investigate whether a relationship exists among fracture permeability, fracture orientation, and the state of stress in situ.

STUDY APPROACH

To examine the relationship among in-situ stress, fractures, and permeability, one needs a relatively complete picture of subsurface conditions that is rarely available. For example, it is relatively straightforward to locate and determine the orientation of large-scale fractures and faults by using borehole image data (e.g., Seeburger and Zoback, 1982; Paillet et al., 1987; Pezard et al., 1988). However, detailed knowledge of the orientation and magnitude of in-situ stresses is needed to determine if such features are potentially active faults, and detailed flow-meter (Hess, 1986) or temperature (Cornet, 1989) measurements are needed to determine if individual fracture or fault planes are relatively permeable. We report here three case studies where these data are available.

The Cajon Pass scientific drill hole penetrated 3.5 km into granites and granodiorites near San Bernardino, California, ~4 km from the San Andreas fault. An overview of the geologic setting at the Cajon Pass drill hole is given by Zoback et al. (1988) and Silver and James (1988). The stress state at Cajon Pass is transitional between strike-slip and normal faulting (e.g., $\phi \simeq 1.0$, where ϕ defines the relative magnitude of the intermediate principal stress: $[S_2 - S_3]/[S_1 - S_3]$) as indicated by both local geology (Weldon and Springer, 1988) and in-situ stress measurements (Zoback and Healy, 1992).

The Long Valley exploratory well was drilled >2 km into rhyolites and tuffs within the resurgent dome of the Long Valley caldera near Mammoth Lakes in east-central California to investigate the structure and evolution of the caldera (Sass et al., 1992). Analyses of well-bore breakouts and earthquake focal-plane mechanisms indicate a strike-slip–normal-slip stress regime in the vicinity of the resurgent dome with northeast-southwest extension and a ϕ value of ~0.7 (Moos and Zoback, 1993).

The third case study is at Yucca Mountain, Nevada, a potential site for construction of a nuclear waste repository located along the western boundary of the Nevada Test Site. Numerous holes have been drilled to provide information about the site and to evaluate subsurface geologic and hydrologic conditions. Borehole televiewer, in-situ stress, and temperature data from one of these holes, USW-G1, were used in this study. Hole USW-G1 was drilled >1.7 km into east-tilted blocks of Miocene volcanic strata. The stress regime at Yucca Mountain indicates normal faulting with S_{Hmax} oriented north-northwest–south-southeast and a ϕ value of 0.3 determined by hydraulic fracturing tests (Stock et al., 1985).

In each study we determined fracture and fault distribution and orientation from analysis of borehole televiewer data using methods described in Barton and Zoback (1992). Well-bore breakout orientations were used to define the orientation of the least horizontal stress (S_{hmin}), and in-situ stress magnitudes were determined by using a variety of methods (see references cited above). The magnitudes of the principal stresses, S_1, S_2, and S_3, were confirmed by analysis of stress rotation induced by slip on active faults in the study boreholes (Barton and Zoback, 1994). Shear (τ) and normal (S_n) stresses on each fracture are

$$\tau = \beta_{11}\beta_{21}S_1 + \beta_{12}\beta_{22}S_2 + \beta_{13}\beta_{23}S_3 \quad (1)$$

and

$$S_n = \beta_{11}^2 S_1 + \beta_{12}^2 S_2 + \beta_{13}^2 S_3, \quad (2)$$

(Jaeger and Cook, 1979), where β_{ij} terms are the direction cosines between the fracture plane and the stress tensor. We used the Coulomb failure criterion (assuming effective stress),

$$\tau = \mu(S_n - P_p), \quad (3)$$

where P_p is the local hydrostatic pore pressure and μ is the coefficient of friction, to determine whether each plane was a potentially active fault. Planes with a ratio of shear to normal stress of ≥ 0.6 are optimally oriented to the stress field for frictional failure (Byerlee, 1978).

In each of the study boreholes, we used precise temperature measurements to detect localized thermal anomalies associated with fluid flow in and out of the borehole along relatively permeable fractures and faults (Hess, 1986; Cornet, 1989). Although such measurements cannot be used to make precise estimates of permeability, they are quite useful in a qualitative sense for indicating which fractures and faults are effective in conducting fluids (see also Drury, 1989).

When a borehole is close to thermal equilibrium with the surrounding rock, heat transfer occurs primarily by thermal conduction, and the temperature gradient in the borehole is a function of thermal conductivity and heat flux. Localized perturbations of well-bore temperatures (similar to the highly idealized anomalies of Fig. 1) will re-

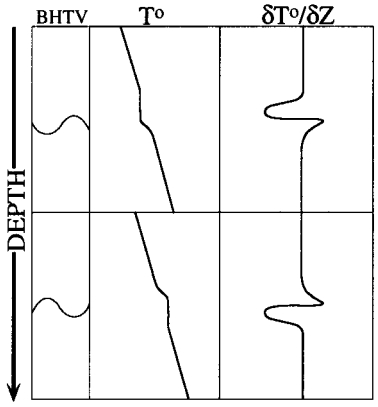

Figure 1. Schematic diagram of thermal anomalies associated with hydraulically conductive fractures intersected by borehole. BHTV is borehole televiewer image, *T*° is temperature and δ*T*°/δ*Z* is differential temperature gradient. Upper part illustrates effect of relatively cold fluid entering well bore from fracture and flowing down well. Similar profile will result if warm fluid flowing up well bore exits at fracture. Effect of warm fluid entering borehole or cold fluid leaving borehole is illustrated in lower part.

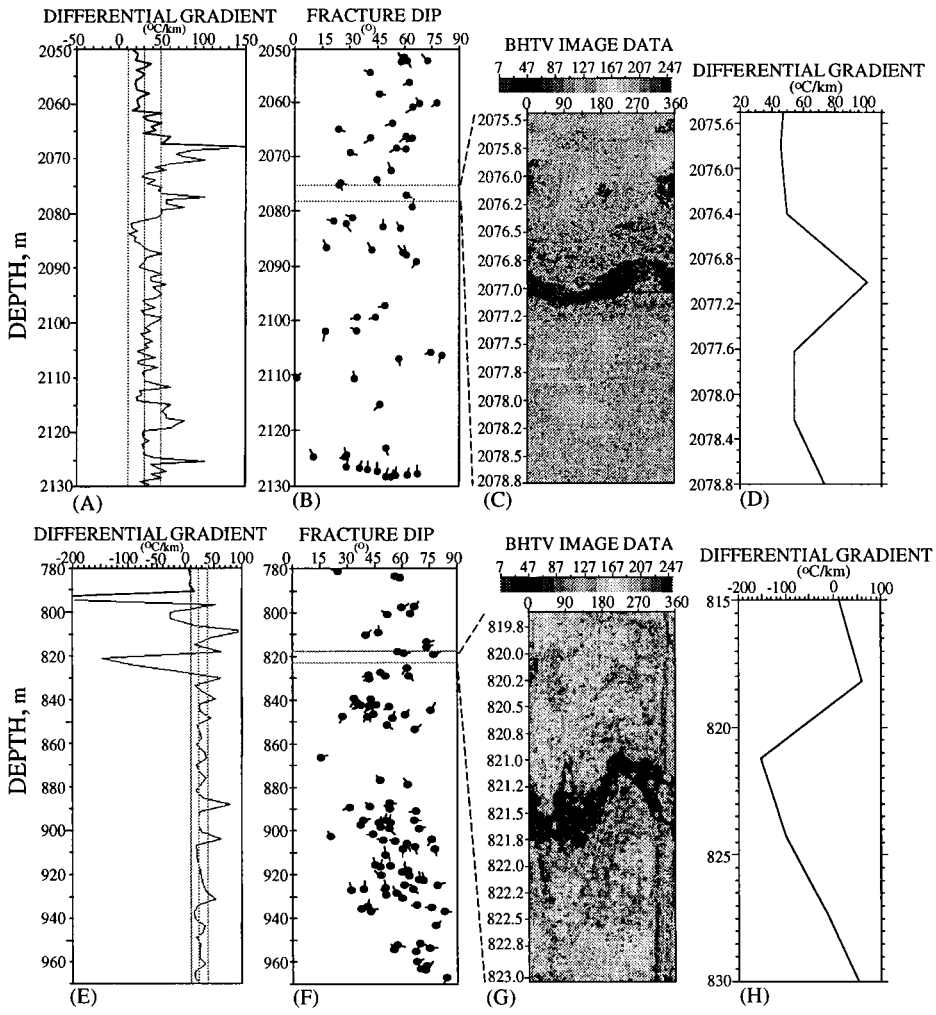

Figure 2. Temperature-gradient profile (A) and fracture data (B) from Cajon Pass borehole over interval 2050 to 2130 m. View of BHTV data (C) near 2077 m showing large natural fracture corresponding to anomaly in temperature gradient at this depth (D). Temperature-gradient profile (E) and fracture data (F) from Long Valley borehole over interval 780 to 980 m. Tadpole "tails" in B and F give fracture-dip direction. View of BHTV (G) data near depth of 821 m shows large natural fracture corresponding to anomaly in temperature gradient at this depth (H).

sult from localized fluid flow into or out of the borehole and can be detected by precision temperature logging. Fractures or faults that correlate in depth with these localized temperature perturbations are therefore considered to be hydraulically conductive.

The idealized temperature anomalies shown in Figure 1 illustrate only the effect of interactions between the fractures and the well bore itself. These simplified profiles may be complicated by several factors including the presence of multiple fractures and the resulting hydrologic interactions. Also, near-vertical fractures produce flow parallel to the borehole, resulting in a near-isothermal temperature profile along the fracture trace. Intervals of near-constant temperature with depth are not observed in the study temperature data. Further, the study boreholes are drilled vertically; consequently, few vertical fractures are intersected. Thus, flow parallel to the borehole along near-vertical fractures does not appear to be a common occurrence in the boreholes studied.

Although the sensitivity of the probes used to record the precision temperature data used in this study is ±20 mK, the sampling interval is 0.305 m (1 ft). Therefore, variations in temperature associated with variations in fracture infilling materials or changes in lithology at a scale finer than the 0.305 m sampling interval will not be detected.

Examples of the types of data used in this study are shown in Figure 2; these are portions of the temperature-gradient profiles over the interval 2050 to 2130 m in the Cajon Pass research borehole and 780 to 970 m in the Long Valley exploratory well (Figs. 2, A and E). The Cajon Pass profile shows several temperature anomalies indicative of heat loss (e.g., at 2068 and 2077 m) whereas many anomalies in the section of the Long Valley profile appear to indicate heat gain (e.g., at 802 and 821 m). Adjacent to the temperature-gradient profiles are plots of the distributions and orientations of natural fractures over the same depth intervals. A closer look at the interval 2075.5 to 2078.8 m of the Cajon Pass borehole afforded by televiewer image data (Fig. 2C) shows a natural fracture crosscutting the borehole at 2077 m. The corresponding interval of the temperature-gradient profile (Fig. 2D) indicates a clear association between the depth of the fracture and that of a local temperature-gradient anomaly. A similar correlation between the temperature-gradient profile and the image data of the Long Valley borehole is evident in Figures 2, G and H.

To investigate the correlation between localized temperature anomalies and specific permeable fractures, we isolated the obviously hydraulically conductive fractures in the study boreholes on the basis of temperature-gradient data. Temperature logs commonly contain some degree of noise due to the extremely high sensitivity of the probe. To eliminate the exaggeration of this noise in the temperature-gradient profiles, we applied a five-point average-depth smoothing to the temperature data corresponding to a moving window of 1.5 m. The temperature profiles for both the Cajon Pass and Nevada Test Site boreholes could be fit by a constant temperature gradient with depth (e.g., 30 °C/km and 25 °C/km, respectively), indi-

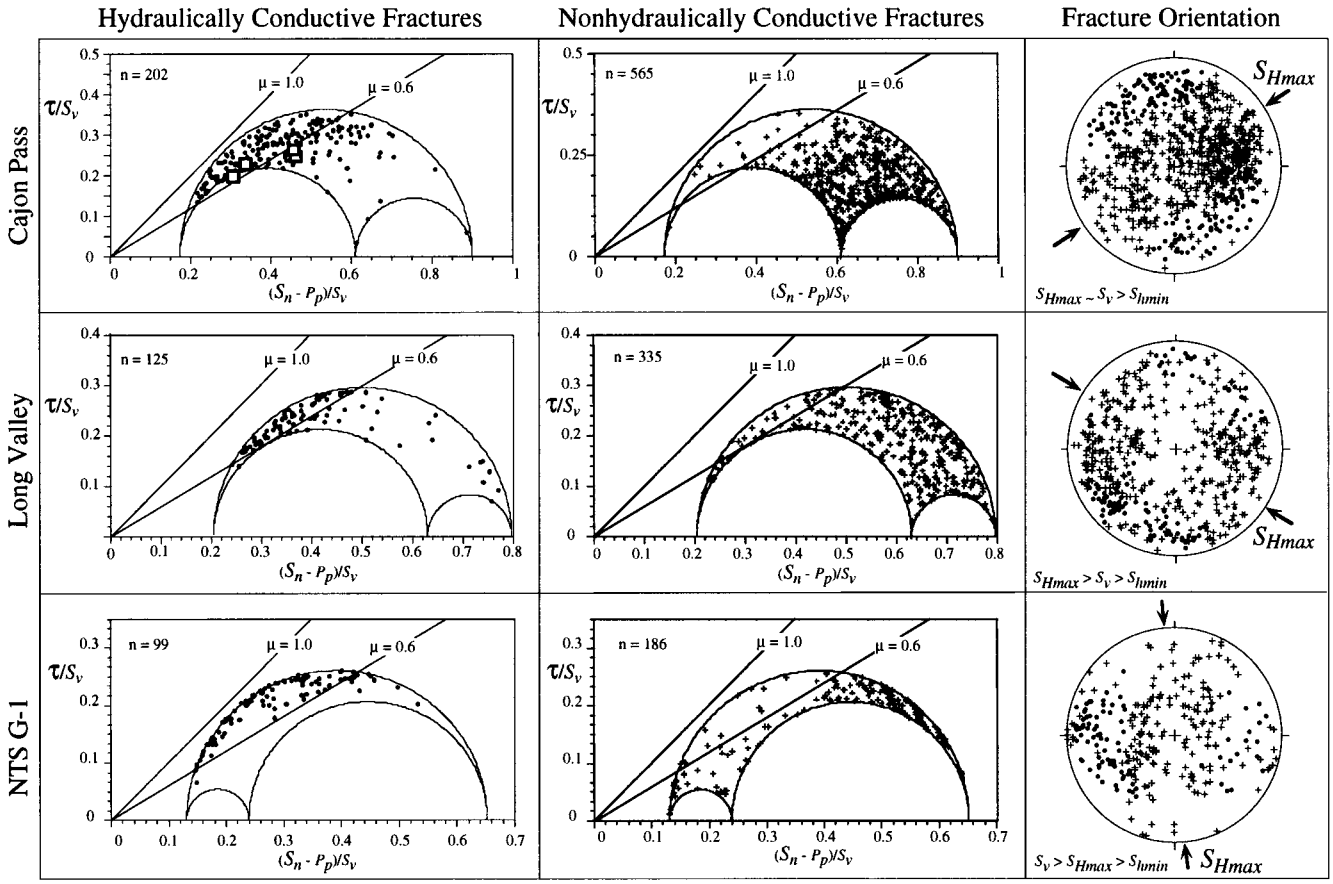

Figure 3. Normalized shear vs. effective normal stress for hydraulically conductive (left column) and nonhydraulically conductive (center column) fractures based on precision temperature logs (refer to Jaeger and Cook, 1979, p. 28, for details of construction of these diagrams). Open squares in upper left plot show stress state calculated for fractures in Cajon Pass borehole where flow was indicated by direct flow tests. Right column shows lower-hemisphere stereographic projections of poles to fracture planes for hydraulically conductive (solid circles) and nonhydraulically conductive (plus signs) planes.

cating that these measurements were made after the boreholes had reached thermal equilibrium and that heat flow was primarily conductive. Nonequilibrium temperature conditions in the Long Valley borehole required the computation of a local average gradient. Temperature anomalies were selected by establishing a temperature-gradient cutoff value above which the largest anomalies were clear. Reference lines for Cajon Pass at 30 ± 20 °C/km and 25 ± 15 °C/km for Long Valley indicate the average temperature gradients. Where repeat temperature logs are available, these relatively large anomalies in the temperature gradient are found to persist but diminish with time (Lachenbruch and Sass, 1988).

Fractures detected with televiewer image data within ±1.0 m of an obvious temperature anomaly were assumed to be responsible for fluid flow at the anomaly. If more than one fracture was present within ±1.0 m of the temperature anomaly, we selected the dominant fracture orientation (the statistical mode). Ambiguity in fracture orientation was unresolved for only 5% to 10% of the temperature anomalies in all cases. Because of the resolution limitations of the televiewer, small fractures (apparent apertures of <10 mm) may go undetected (see Barton and Zoback, 1992, for a discussion of tool resolution). However, temperature anomalies could be associated with fractures in 93%–95% of cases in the three studies. Thus, a relatively small number of hydraulically conductive fractures appear to have been missed by the imaging tool.

STUDY RESULTS

The fracture and fault data in three-dimensional Mohr representations (shear vs. effective normal stress normalized by the vertical stress) are shown in the first two columns of Figure 3. As indicated by the Coulomb failure lines for $\mu = 0.6$ and $\mu = 1.0$ in the left column, most of the hydraulically conductive fractures (~70%–80%) appear to be critically stressed, potentially active faults in frictional equilibrium with the in-situ stress field. The middle column in Figure 3 reveals that most fractures where no flow is indicated are not critically stressed. For each 1-m-depth interval where no temperature anomaly was detected, we again selected a fracture orientation representing the dominant trend of fractures in that interval. Note that the majority of fractures not associated with temperature anomalies clearly lie below the Coulomb failure curve and therefore do not appear to be critically stressed shear fractures.

The right column of Figure 3 compares poles of the population of conductive fractures to the orientations of nonconductive fractures in lower-hemisphere equal-area stereonets. In each study case, the orientations of conductive fractures are distinct both from the orientation of the total fracture population and the orientations of nonconductive fractures.

Although it is not possible to determine the extent of fracture conductivity away from the borehole from the temperature and image data alone, direct flow tests do measure fracture conductivity at a distance from the borehole. Two direct flow tests were conducted in the Cajon Pass drill hole over the intervals from 1829 to 1905 and

1829 to 2115 m (Kharaka et al., 1988). Results indicate that ~80% of the inflow originates from a single fracture near 2077 m. Other major fractures possibly contributing to flow (detected from these flow tests, Stoneley and refracted wave amplitudes, and drilling breaks; Barton and Moos, 1988) are near depths of 1840, 1940, and 2030 m. The computed shear and normal stress for these conductive fractures are plotted as open squares in the top left Mohr diagram of Figure 3. In each case, they plot over or near the Coulomb failure line for $\mu = 0.6$. This result provides direct evidence of flow away from the well-bore associated with planes optimally oriented to the stress field for frictional failure.

Experimental and theoretical studies of relations between permeability and shear displacement show that the permeability of shear fractures is strongly affected by fracture roughness and aperture (Brown, 1987). Dilatancy (pore-volume expansion from the formation of microcracks) is one possibly important phenomenon affecting fault conductivity under shear deformation (Maini, 1971; Makurat, 1985). Teufel (1987) recognized the localized development of microfracture zones immediately adjacent to the sliding surface of sandstone samples under triaxial compression; this finding suggested that a narrow channel of high permeability parallel to the fracture might develop during shear deformation (Antonellini and Aydin, 1994). Microfracture zones were observed by Tchalenko (1970) to form during direct shear tests of intact rock as en echelon fractures that coalesce into a fault plane. The degree to which dilatancy or active shear displacement causes critically stressed faults to maintain permeability is not known. If, during deformation, porosity and permeability are increased as a result of dilatancy or shear displacement, one fundamental criterion for fluid flow along faults is that the fault be critically stressed and close to frictional failure.

Many factors contribute to a fracture's bulk permeability, such as its aperture and degree of remineralization. Exceptions to the overall correlation between critically stressed and hydraulically conductive fractures seen in Figure 3 may largely be the result of these factors. An investigation of well-bore image data and fine-scale fluid-flow measurements made in conjunction with complete core analysis would serve to elucidate the importance of these geologic factors to in-situ fluid flow. The resolution limits of the imaging tool and temperature probe discussed above will also contribute to the scatter in the statistical methods of this study. It is clear, however, that even without knowledge of the specific details of individual fracture characteristics, and even with the inherent sampling limitations of the logging tools, a remarkable correlation exists between critically stressed faults and hydraulic conductivity in highly fractured crystalline rock.

ACKNOWLEDGMENTS

We thank Colin Williams and John Sass of the U.S. Geological Survey, Menlo Park, California, for helpful discussions and for providing precision temperature data for the study drill holes. We thank Steve Hickman, Stuart Rojstaczer, Fred Paillet, and Ian Main for helpful discussions and comments.

REFERENCES CITED

Antonellini, M., and Aydin, A., 1994, Effect of faulting on fluid flow in porous sandstones: American Association of Petroleum Geologists Bulletin, v. 78, p. 355–377.

Barton, C. A., and Moos, D., 1988, Analysis of macroscopic fractures in the Cajon Pass Scientific Drillhole: Geophysical Research Letters, v. 15, p. 1013–1016.

Barton, C. A., and Zoback, M. D., 1992, Self-similar distribution and properties of macroscopic fractures at depth in crystalline rock in the Cajon Pass scientific drill hole: Journal of Geophysical Research, v. 97, p. 5181–5200.

Barton, C. A., and Zoback, M. D., 1994, Stress perturbations associated with active faults penetrated by boreholes: Journal of Geophysical Research, v. 99, p. 9373–9390.

Brown, S. R., 1987, Fluid flow through rock joints: The effect of surface roughness: Journal of Geophysical Research, v. 92, p. 1337–1347.

Byerlee, J., 1978, Friction of rocks: Pageoph, v. 116, p. 615–626.

Cornet, F. H., 1989, Survey by various logging techniques of natural fractures intersecting a borehole: Proceedings, International Symposium on Borehole Geophysics for Mining, Geotechnical and Groundwater Applications, 3rd, v. II, p. 559–569.

Drury, M. J., 1989, Fluid flow in crystalline crust: Detecting fractures by temperature logs, *in* Beck, A. E., et al., eds., Hydrogeological regimes and their subsurface thermal effects: International Union of Geodesy and Geophysics, Geophysical Monograph 47, v. 2, p. 129–136.

Hess, A. E., 1986, Identifying hydraulically-conductive fractures with a low-velocity flowmeter: Canadian Geotechnical Journal, v. 23, p. 69–78.

Jaeger, J. C., and Cook, N. G. W., 1979, Fundamentals of rock mechanics (third edition): New York, Chapman and Hall, p. 28–30.

Kharaka, Y. Y., White, L. D., Ambats, G., and White, A. F., 1988, Origin of subsurface water at Cajon Pass, California: Geophysical Research Letters, v. 15, p. 1049–1052.

Lachenbruch, A. H., and Sass, J. H., 1988, The stress–heat flow paradox and thermal results from Cajon Pass: Geophysical Research Letters, v. 15, p. 981–984.

Long, J. C. S., Karasaki, K., Davey, A., Peterson, J., Landsfeld, M., Kemeny, J., and Martel, S., 1991, An inverse approach to the construction of fracture hydrology models conditioned by geophysical data: International Journal of Rock Mechanics, Mineral Science & Geomechanics Abstracts, v. 28, p. 121–142.

Maini, Y. N. T., 1971, In situ hydraulic parameters in jointed rock: Their measurement and interpretation [Ph.D. thesis]: London, Imperial College, University of London, 312 p.

Makurat, A. N., 1985, The effect of shear displacement on the permeability of natural rough joints, *in* Hydrogeology of rocks of low permeability: International Association of Hydrogeologists Memoir 17, p. 99–106.

Moos, D., and Zoback, M. D., 1993, State of stress in the Long Valley caldera, California: Geology, v. 21, p. 837–840.

Paillet, F. L., Hess, A. E., Cheng, C. H., and Hardin, E., 1987, Characterization of fracture permeability with high-resolution vertical flow measurements during borehole pumping: Ground Water, v. 25, p. 28–40.

Pezard, P. A., Anderson, R. N., Howard, J. J., and Luthi, S. M., 1988, Fracture distribution and basement structure from measurements of electrical resistivity in the basement of the Cajon Pass scientific drillhole, California: Geophysical Research Letters, v. 15, p. 1021–1024.

Pollard, D., and Aydin, A., 1988, Progress in understanding jointing over the past century: Geological Society of America Bulletin, v. 100, p. 1181–1204.

Sass, J. H., Rundle, J. B., and Eichelberger, J. C., 1992, Probing the center of Long Valley caldera, California: Proceedings, International Geological Congress, 29th, Kyoto, Japan, Abstracts, v. 3, p. 837.

Seeburger, D. A., and Zoback, M. D., 1982, The distribution of natural fractures and joints at depth in crystalline rock: Journal of Geophysical Research, v. 87, p. 5517–5534.

Silver, L. T., and James, E. W., 1988, Geologic setting and lithologic column of the Cajon Pass deep drillhole: Geophysical Research Letters, v. 15, p. 941–944.

Stock, J. M., Healy, J. H., Hickman, S. H., and Zoback, M. D., 1985, Hydraulic fracturing stress measurements at Yucca Mountain, Nevada, and relationship to the regional stress field: Journal of Geophysical Research, v. 90, p. 8691–8706.

Tchalenko, J. S., 1970, Similarities between shear zones of different magnitudes: Geological Society of America Bulletin, v. 81, p. 1625–1640.

Teufel, L. W., 1987, Permeability changes during shear deformation of fractured rock, *in* 28th Symposium on Rock Mechanics: Rotterdam, Netherlands, A. A. Balkema, p. 473–480.

Weldon, R. J., and Springer, J. E., 1988, Active faulting near the Cajon Pass well, southern California: Geophysical Research Letters, v. 15, p. 993–996.

Zoback, M. D., and Healy, J. H., 1992, In situ stress measurements to 3.5 km depth in the Cajon Pass scientific research borehole: Journal of Geophysical Research, v. 97, p. 5039–5057.

Zoback, M. D., Silver, L. T., Henyey, T., and Thatcher, W., 1988, The Cajon Pass scientific drilling experiment: Geophysical Research Letters, v. 15, p. 933–936.

Manuscript received February 27, 1995
Revised manuscript received May 2, 1995
Manuscript accepted May 10, 1995